ORGANOMETALLICS

pubs.acs.org/Organometallics Article

Reversible Photoisomerization in a Ru *cis*-Dihydride Catalyst Accessed through Atypical Metal—Ligand Cooperative H₂ Activation: Photoenhanced Acceptorless Alcohol Dehydrogenation

Paul M. Fanara, Vipulan Vigneswaran, Parami S. Gunasekera, Samantha N. MacMillan, and David C. Lacy*



Cite This: Organometallics 2022, 41, 93-98



ACCESS

Metrics & More

Article Recommendations

Supporting Information

ABSTRACT: Dehydrohalogenation of pyridine-derived pincer ruthenium complexes often leads to dearomatized moieties, such as in Milstein's PNN-Ru(CO)(Cl)(H) (1Py) catalyst. Thus, we were surprised to find an aromatized κ^3 -N,C,P binding mode in the lutidine-derived bidentate analogue [{LutP'}Ru(CO)(H)(PPh_3)] (2), instead of a dearomatized compound, upon dehydrohalogenation of [{LutP}Ru(CO)(Cl)(H)(PPh_3)] (1). The reaction of 2 with H₂ results in the formation of the *cis*-dihydride [{LutP}Ru(CO)(H)₂(PPh₃)] (3), and labeling studies confirm cooperative metal—ligand activation. 3 exhibits reversible photoisomerization,

forming another cis-dihydride isomer (4) upon irradiation. The lability of 4 toward ligand substitution was leveraged to demonstrate photoenhanced H_2 production via acceptorless alcohol dehydrogenation. Labeling studies implicate metal—ligand cooperative (MLC) processes during the photocatalytic reaction, but they appear to be off-path processes on the basis of our mechanistic study of the system. The latter emphasizes that aromatization/dearomatization may not be necessary for acceptorless transformations, which is generally consistent with several contemporary studies on analogous Ru catalysts.

■ INTRODUCTION

Transition-metal hydrides (TMH) have rich photochemical properties. In some cases, these enable photoassisted catalysis. Examples of these key properties include light-induced M–H homolysis, reductive elimination of H_2 from *cis*-dihydrides, altered chemical properties (e.g., pK_a , hydricity, etc.), 4.5 and photoisomerization. If these processes are chemically reversible, they can benefit the system by preventing the formation of off-path photogenerated thermodynamic sinks and in principle could be harnessed as a photoswitch. Phenomenologically, the *cis*-dihydride motif is best suited to this end because it tends to exhibit reversible photochemical properties. I

During the course of our studies, we discovered the Ru alcohol dehydrogenation precatalyst 1 with the on-path *cis*-dihydride complex 3 exhibiting reversible photochemical reactivity and describe this discovery herein. The *cis* motif was accessed through an atypical mode of metal–ligand cooperative H_2 activation by the key intermediate 2. The unusual coordination chemistry of 2 that previous to this study was unexpected adds to the developing story of aromatization/dearomatization metal–ligand cooperativity (MLC) in catalytic cycles (Scheme 1).^{8–10} Furthermore, the reversible photochemistry of 3 enabled photoenhanced H_2 production from various alcohols using very mild reagents and conditions (rt, λ > 345 nm) with implications in the area of acceptorless MLC alcohol dehydrogenation. ^{11–14}

Scheme 1. (Top) Conventional Metal—Ligand Cooperativity (MLC) with Non-Noyori-type Pyridine-Based Ru(II) Catalysts and (Bottom) Atypical MLC Described in This Study

dearomatization/aromatization metal-ligand cooperativity (MLC)

atypical MLC (this work)

Received: November 22, 2021 Published: December 16, 2021



RESULTS AND DISCUSSION

In an earlier report detailing the synthesis and characterization of $[\{LutP\}Ru(CO)(H)(Cl)(PPh_3)]$ (1), we briefly investigated its reaction with KOtBu and initially hypothesized a prototypical dearomatized bidentate binding mode for the product **2b** analogous to **2Py**. However, the product exhibited unusual sensitivity to water, and we did not pursue it further at the time. Upon reinvestigation, we discovered that activation of **1** with 1 equiv of K[N(SiMe₃)₂] in cold (-35 °C), very dry THF or KOtBu in dry benzene, affords the highly moisture sensitive amber-colored species **2** (Scheme 1), whose X-ray crystal structure contains a unique κ^3 -N,C,P binding mode (Figure 1).

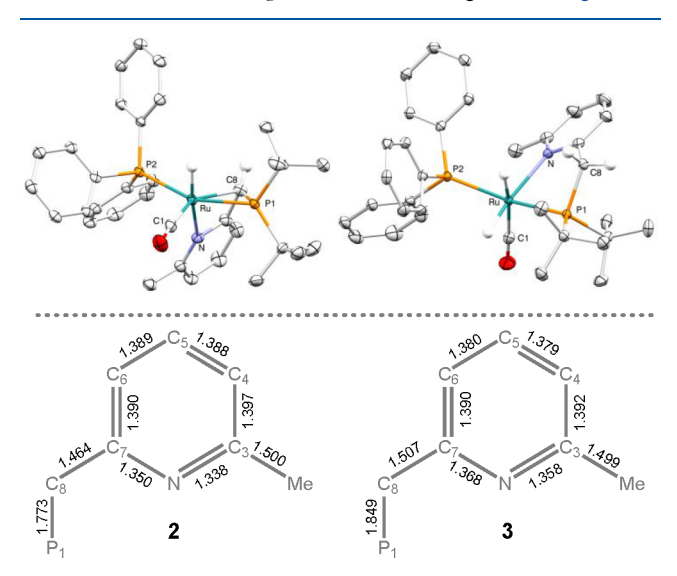


Figure 1. (top) XRD molecular structures of **2** (left) and **3** (right) with ellipsoids at the 50% probability level. Except for the RuH and methine/methylene CH atoms, hydrogen atoms have been removed for clarity. Selected bond distances (Å) and angles (deg) for **2**: Ru-N = 2.196(2); Ru-C8 = 2.309(2); Ru-P1 = 2.2684(6); Ru-P2 = 2.3419(7); Ru-C1 = 1.845(3); Ru-H = 1.53(3); C1-Ru-C2 = 150.4; P1-Ru-P2 = 149.9; C1-Ru-N = 61.8. Selected bond distances (Å) and angles (deg) for **3**: Ru-N = 2.277(2); Ru-P2 = 2.3133(4); Ru-P1 = 2.2960(4); Ru-C1 = 1.887(2); P1-Ru-P2 = 154.8°; C1-Ru-N = 103.4°. (bottom) Distances in the pyridine ring and phosphine arm for **2** and **3**.

Importantly, the κ^3 -N,C,P binding mode remains intact in solution, as evidenced from $^1\text{H}-^1\text{H}$ ROESY NMR correlations and $^1\text{H}/^{13}\text{C}$ coupled HSQC NMR spectroscopy (Figures S1–S8). The salient NMR features of **2** are the methine CH resonances in the ^1H and $^{13}\text{C}\{^1\text{H}\}$ NMR spectra at 1.78 ppm (^2CH , ^2CH , ^2CH) and 12.41 ppm (^2CH , ^2CH), respectively. Additionally, the Ru-H resonance in the ^1H NMR appear at ^2CH 1.6 ppm (^2CH 1, ^2CH 2, ^2CH 3, ^2CH 3, ^2CH 3, ^2CH 4, ^2CH 3, ^2CH 4, ^2CH 5, ^2CH 6, ^2CH 7 and ^2CH 6, ^2CH 9 and ^2CH 9 pm (^2CH 1). For comparison, the analogous groups in ^2CH 9 have resonances at ^2CH 1 and ^2CH 2 ppm, all of which are consistent with the dearomatized mode ($^2\text{Cheme}$ 1). Spectroscopic features similar to those for **2** for "armbound" type binding modes have been observed, ^2CH 9 but not for ruthenium complexes with pyridine-derived ligands that can undergo reversible aromatization/dearomatization.

Reaction of 2 with H_2. The unusual binding mode of **2** was of interest to us, as we hypothesized that the Ru–C bond would be highly reactive toward H_2 and H_2 donors such as 2-propanol. Indeed, when a benzene solution of **2** was exposed to an atmosphere of H_2 , an immediate color change from amber to

light yellow occurred and NMR analysis revealed the quantitative formation of a cis-dihydride, 3 (Scheme 2).

Scheme 2. Reaction of 2 with H₂

Similarly, 2 reacts quantitatively with 2-propanol (3 equiv) to form 3 and 1 equiv of acetone. An X-ray crystallographic characterization revealed the *cis*-dihydride motif, and 2D NMR and $^1\text{H}-^1\text{H}$ ROESY spectroscopic characterization confirmed that its solution-state structure is identical (Figures S9–S13). Subjecting 3 to vacuum at elevated temperatures (60 °C) or excess acetone (rt) resulted in no conversion to 2. More forcing conditions (110 °C) resulted in trace formation of 2 along with [(CO)(PPh₃)₃Ru(H)₂] and other unidentified byproducts (Figure S26). This stability toward ketones and the inability to lose H₂ is in contrast to previous reports with Milstein's dihydride complex, 3Py, which spontaneously converts to 2Py with loss of H₂ at room temperature. ^{7,8,15}

When D_2 was used to prepare 3, deuterium incorporation occurred at both ruthenium and the ligand, consistent with an MLC activation of H_2 (Scheme 3). The mixture of isotopomers

Scheme 3. Reaction of 2 with D₂

is best represented pictorially in Scheme 3 (2 H NMR, Figure S18) and is generally consistent with what others have observed. 21 Notably, H_2 and HD were observed in the 1 H NMR spectrum when 2 was treated with D_2 , indicating exchange with free dihydrogen (Figure S19). While they were not completely eliminated, the presence of H_2 and HD was significantly reduced when light was rigorously excluded (Figure S20). As such, we hypothesized that photochemical processes are responsible.

Photochemistry of 3. We tested this hypothesis with broad-band irradiation of 3 with a Xe arc lamp (100 W), which caused a color change of the solution to orange-red. ¹H NMR spectroscopy reveals the new dihydride species 4 that quantitatively converts back to 3 in a few hours (Scheme 4); this process can be repeated several times, even under static vacuum. The ¹H NMR spectrum of 4 contains two hydride resonances at -5.13 ppm (dd, J = 101, 25 Hz) and -6.09 ppm (dd, J = 92, 17 Hz), consistent with a phosphine trans and cis to each hydride, respectively (Figure S14). The ³¹P{¹H} NMR spectrum indicates a cis conformation of the PtBu₂ and PPh₃ ligands, as the resonances at 77.3 and 42.7 ppm are doublets with $J_{\rm PP} = 11$ Hz, respectively (Figure S15). $^{1}{\rm H} - ^{1}{\rm H}$ ROESY NMR of 4 shows exchange coupling between the two hydride resonances. Additionally, the hydride resonance at -6.09 ppm has an NOE to one of the PtBu₂ resonances at 1.30 ppm. The hydride

Scheme 4. Reversible Photochemistry of 3

resonance at -5.13 ppm exhibits NOE to the PPh₃ and methyl resonances at 7.72 and 2.56 ppm, respectively (Figure S16). Together with FTIR-ATR spectroscopy (Figure S17), the NMR data enable confident assignment of the structure of 4 as shown in Scheme 4.

The stability of 4 was monitored with ^1H NMR spectroscopy, and it quantitatively decayed with $t_{1/2}=1.90\pm0.04\,\text{h}$ (rt) back to 3 under N₂ (Figures S29 and S30). The decay was unaffected by static vacuum: $t_{1/2}=1.80\pm0.14\,\text{h}$ (rt) (Figures S23 and S24). When the photolysis of 3 was carried out under an atmosphere of H₂, the same process occurred, except that the decay of 4 to 3 was slower ($t_{1/2}=3.38\pm0.08\,\text{h}$) (Figures S31 and S32). This photogeneration of 4 and isomerization to 3 could be repeated several times (attempted up to three times) without any noticeable decomposition or loss of function.

While 3 is unreactive toward CO, 4 does not form when 3 is irradiated in the presence of CO; instead, the carbonylated product 8 is formed (Scheme 5 and Figures S38 and S39).

Scheme 5. Summary of Decomposition Reaction Photolysis under CO or with Free PPh₃

Similarly, 3 does not react with free PPh₃, but after a 2 h irradiation of a mixture of 3 and PPh₃, 4 is the major product along with the byproducts $[(CO)(PPh_3)_3Ru(H)_2]$ (6), $[(PPh_3)_3Ru(H)_4]$, 8, free ligand, and other unidentified species (Figure S37) (Scheme 5). These suggest the possibility that 3 photoeliminates H₂ or another ligand but rapidly recombines to form 4, similar to what others have observed. Alternatives include a photoinduced unimolecular trigonal "twist". For the conversion of 4 back into 3, we hypothesize a unimolecular trigonal twist, 22,25 since the isomerization half-life was the same under N₂ and vacuum.

Exchange of H₂ with the Hydrides of 4. Irradiation of an NMR sample of 3 under an atmosphere of D₂ results in the hydride resonances washing out in the ¹H NMR spectrum with concomitant reappearance in the ²H NMR spectrum. Deuterium incorporation into the ligand was *not* observed (Figures S21 and S22). These results suggest an exchange is taking place between the hydrides of 4 and free D₂. A ¹H–¹H ROESY NMR spectrum of 4 under H₂ confirms the exchange between both hydride resonances and free H₂ (Figure S16). A variable-temperature NMR and line-broadening analysis fur-

nished activation parameters of $\Delta H^{\ddagger} = 24.0 \pm 1.2$ kcal mol⁻¹ and $\Delta S^{\ddagger} = 22.9 \pm 3.4$ cal K⁻¹ mol⁻¹ (Figures S35 and S36). We propose that the reaction is an interchange ligand substitution between 4 and H₂ with either PPh₃ or CO as the leaving group to form complex 5 (Scheme 4), although a dissociative ligand substitution mechanism is possible.

The proposed presence of 5 explains two important observations. First, the appearance of both HD and H_2 when 3 or 2 was treated with D_2 and exposed to light cannot be easily explained without the presence of a tetra- or trihydride intermediate, which are known to mediate the H_2 isotope exchange reaction. Second, it also explains how the isomerization of 4 to 3, although not affected by vacuum, is slowed by the presence of H_2 : the off-path equilibrium between 4 and H_2 allows for this to happen.

We suspect there is also a thermal reaction between H_2 and 3, because if 3 and D_2 are left to stand in the dark for several days, the hydride resonances eventually wash out and reappear in the 2H spectrum (Figure S23). The ligand exchange between 4 and H_2 is rapid (as evidenced from the line broadening) in comparison to the ligand exchange between 3 and H_2 . This enhanced lability of 4 is important for enabling catalysis.

Photoenhanced Catalysis. Our previous investigation with 1 involved testing different ligand variants in alcohol dehydrogenation. In that case, and also most others, tatalytic behavior was not achieved unless reactions were carried out at elevated temperatures. However, we intuited that complexes such as 3, having reversible photochemistry, might be amenable to rt photocatalytic alcohol dehydrogenation, akin to what has been observed in certain cases, accessed through photoisomerization to the more labile species 4. We tested several simple alcohols using 3 with irradiation from a Xe arc lamp (100 W, 345 nm cutoff filter) and achieved catalytic turnover at rt (Figure 2 and Table 1). Under the same conditions but with the

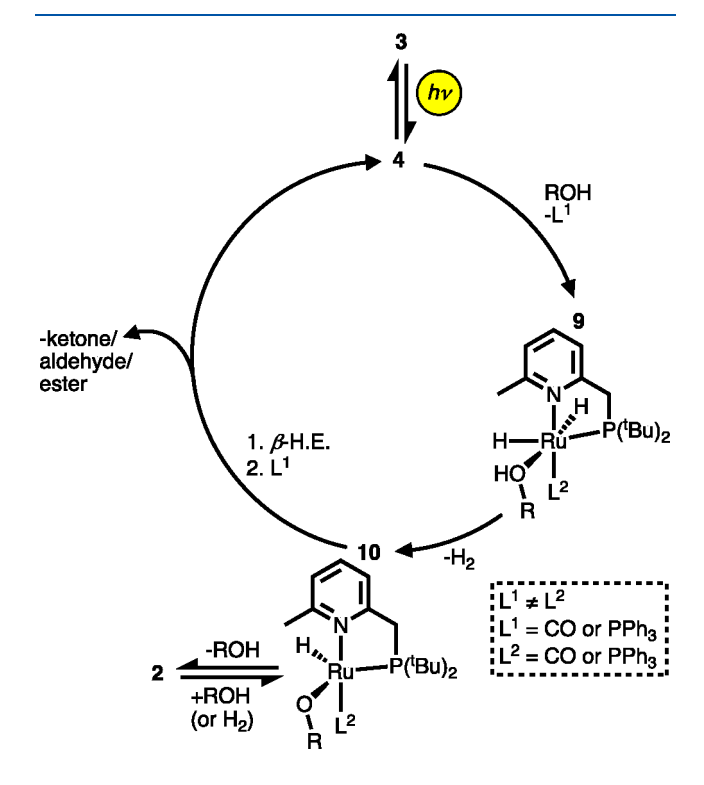


Figure 2. Proposed mechanism for photocatalysis for 2-propanol dehydrogenation.

Table 1. Results of Photocatalysis

alcohol
$$\frac{\text{cat, } hv}{4 \text{ h, 23 °C, neat}}$$
 carbonyl-compound + H₂

entry	alcohol	cat.	product	H_2 relative to cat. ^b (after 12 h) (%)
1	MeOH	3	H_2CO^c	270 (400)
2	EtOH	3	ethyl acetate ^c	640 (1000)
3	1-PhEtOH	3	acetophenone	640 (1100)
4	iPrOH	3	acetone	300 (510)
5	<i>i</i> PrOH	3^d	acetone	27
6	iPrOH	1	acetone	78
7	iPrOH	6	acetone	33
8	<i>i</i> PrOH	7	acetone	28

^aConditions unless specified otherwise: 2 mL of alcohol, 0.02–0.04 mol % of catalyst, 200 μL of benzene, under N₂, irradiation with a Xearc lamp (100 W) with a 345 nm cutoff filter for 4 h. The yield of H₂ was determined by GC. See the Supporting Information for the methodology in product identification. Abbreviations: **6**, [CO-(PPh₃)₃Ru^{II}(H)₂]; 7, [(Cl)(CO)(PPh₃)₃Ru(H)]. 1-PhEtOH, 1-phenylethanol. ³⁰ ^bAverage of three runs. ^cTrace CO observed. ^dDark.

exclusion of light, only substoichiometric H_2 was formed (e.g., 27% of H_2 relative to 3 from 2-propanol; Table 1, entry 5). A larger-scale photolysis reaction was conducted open to a bubbler and resulted in conversions comparable to those of the closed system.

As was noted, $[CO(PPh_3)_3Ru^{II}(H)_2]$ (6) was observed as a product when 3 was irradiated in the presence of free PPh₃, and since 6 is a known alcohol dehydrogenation catalyst, we performed a control reaction but found that it was not the active catalyst. Namely, a control reaction with 6 gave 10% of H_2 in the dark, and 33% on irradiation, with the hydrogen observed simply being the result of the known photoelimination of H_2 from 6. This is not surprising, as catalytic dehydrogenation from 6 requires high temperatures (110 °C). Likewise, (Cl)(CO)-(PPh₃)₃Ru(H) (7) and 1 were not catalysts.

Mechanism of Photoenhanced Dehydrogenation. The two accepted conventional paths for acceptorless alcohol dehydrogenation are the inner-sphere and outer-sphere mechanisms, and these have been discussed at length. We recently provided a rationale for a favored inner-sphere path, consistent with other literature, and lately it has been recognized that MLC steps need not be invoked. In addition to the experimental results described herein, these factors influenced our proposed mechanistic scheme (Figure 2). We recognize that the outer-sphere path is also possible, but we will not discuss it further.

Except for MeOH, postirradiated benzene solutions with 10–20 equiv of alcohol contain 3 and 4 as the major species. In MeOH, the carbonylated byproduct 8 is the major component (tentative structure shown in Scheme 5 and Figure S45).

The first step in photoenhanced alcohol dehydrogenation is the reversible photoinduced isomerization of 3 to 4. The salient component of the mechanism is the enhanced lability of PPh₃ and/or CO in 4 because of the *trans* effect of the hydride ligand and/or steric crowding from the *cis*-diphosphine motif. The lability enhancement allows for alcohol coordination and subsequent liberation of H₂ from the proposed intermediate 9. Loss of H₂ from 9 forms the proposed coordinatively unsaturated species 10, which is predisposed to undergo β -hydride elimination and ligand recoordination, re-forming 3 or

4; thus, the dehydrogenation is an inner-sphere mechanism and no MLC steps are necessary.

A shutter-style experiment was performed to determine photoswitchability. Substoichiometric quantities of H₂ were observed when complex 3 was reacted with alcohols in the dark, with catalysis only being observed upon irradiation. When the light was turned off and the solution was placed back in the dark, H₂ liberation returned to its dark-state production rate. However, upon a second irradiation, the on state for H₂ liberation was not fully restored (Figure S51). The substoichiometric H2 formation in the dark in reactions between 3 and alcohols indicates a thermal pathway. Consistent with our previous studies, carrying out the photolysis at elevated temperature improves the yields of H₂ from isopropanol (450% at 40 °C in comparison to 300% at 23 °C). Thus, we propose that the role of light in photocatalysis is only to generate and maintain a steady-state concentration of 4. This supposition comes from our observation that the wavelength requirements for photocatalysis are the same as those required for photoisomerization (Figures S28 and S40). It appears, however, that returning the system to its dark state at high alcohol concentrations is detrimental, likely resulting in decomposition via pathways outlined above (i.e., formation of 6-8).

When 3 was irradiated in C_6D_6 in the presence of d_8 -isopropanol, deuteration occurred on the ligand (Figures S24 and S25). This would seem to indicate an MLC step in the photocatalysis. However, to explain this observation, we propose that 9 or 10 may react to form 2 (or species like it), which undergoes MLC activation of alcohol in an off-path step (Figure 2). Hence, the MLC chemistry observed here is not likely important for turnover, as depicted in Figure 2.

Extension to Other Systems. The catalytic conversions are low in comparison to photocatalytic alcohol dehydrogenation with Wilkinson's catalyst and other photocatalytic systems, 27 but the conditions we used (rt, neat alcohol, $\lambda > 345$ nm) are very mild. A notable example of mild photochemical alcohol dehydrogenation uses a platinum(II) diphosphite complex at rt and with visible light $\lambda = 410$ nm but requires biphasic H_2O and CH_2Cl_2 conditions and a phase transfer reagent. Conventional acceptorless alcohol dehydrogenation uses high temperatures 11,14 or photosensitizers. Hence, achieving unsensitized photocatalysis for H_2 production (i.e., single-component systems) $^{33-37}$ at low temperatures is desirable. One possible means is to take advantage of photoisomerizable *cis*-dihydrides as demonstrated with 3 and 4, and we wondered if this could be extended to other systems.

We considered that [RuHCl(CO)(HN(CH₂CH₂PPh₂)₂)] (i.e., Ru-MACHO), which is a known effective alcohol dehydrogenation catalyst at low temperatures, ^{38,39} might have photoenhanced rt catalysis. Testing this hypothesis indicates that it does not. Specifically, Ru-MACHO (Ph substituted) exhibited TON = 6 (4 h), with or without light, for 2-propanol dehydrogenation in 4 h. This is in contrast to the work with 3, which is very slow at rt in the dark (TON \approx 0.3, 4 h; Table 1, entry 4) in comparison to that on irradiation to generate its more labile isomer 4 (TON = 3, 4 h; Table 1, entry 5), effectively demonstrating the photoenhancement in the new system.

We also tested Milstein's Ru-PNN trans-dihydride 3Py and obtained TON = 1-3 with or without light, but 3Py is known to spontaneously lose H_2 on standing in solution at rt, and we found that even the chlorido precursor to 3Py (i.e., 1Py) produces hydrogen on irradiation in anhydrous benzene; thus, the comparison is rather inconclusive. We also note that

irradiation of Ru-MACHO and **3Py** with broad-band light resulted in solutions containing a multitude of hydride resonances in the 1H NMR spectrum and speciation by $^{31}P\{^1H\}$ NMR was complicated. Therefore, a careful study is necessary to infer the action of light on these systems, which is outside the scope of the current report.

CONCLUSION

Our work with 2, having an atypical mode of MLC, provides new intermediates to consider when MLC is invoked on pyridinederived ligands. Nevertheless, our mechanistic investigation of the catalytic acceptorless alcohol dehydrogenation does not require MLC steps, consistent with a growing body of literature that has de-emphasized the importance of aromatization/ dearomatization in catalytic cycles. The atypical MLC H₂ activation resulted in the formation of a cis-dihydride motif in 3, which in turn exhibited reversible light-induced isomerization, something that is potentially less likely on analogous transdihydride catalysts. The photogenerated labile compound 4 was competent to engage in catalytic rt alcohol dehydrogenation. However, the conversions are low. Certain decomposition pathways for 4 were identified and are possible sources for the poor TON. The photoenhanced catalysis was not observed in related Ru complexes; thus, we suspect that designing systems with reversible photoisomerizations (or other photochemical processes) is vital to using TMHs as photocatalysts.

ASSOCIATED CONTENT

Supporting Information

The Supporting Information is available free of charge at https://pubs.acs.org/doi/10.1021/acs.organomet.1c00648.

Experimental details, methods, and characterization data (PDF)

Accession Codes

CCDC 2091357—2091358 contain the supplementary crystallographic data for this paper. These data can be obtained free of charge via www.ccdc.cam.ac.uk/data_request/cif, or by emailing data_request@ccdc.cam.ac.uk, or by contacting The Cambridge Crystallographic Data Centre, 12 Union Road, Cambridge CB2 1EZ, UK; fax: +44 1223 336033.

AUTHOR INFORMATION

Corresponding Author

David C. Lacy — Department of Chemistry, University at Buffalo, State University of New York, Buffalo, New York 14260, United States; occid.org/0000-0001-5546-5081; Email: DCLacy@ Buffalo.edu

Authors

Paul M. Fanara — Department of Chemistry, University at Buffalo, State University of New York, Buffalo, New York 14260, United States

Vipulan Vigneswaran — Department of Chemistry, University at Buffalo, State University of New York, Buffalo, New York 14260, United States; orcid.org/0000-0002-8780-8592

Parami S. Gunasekera — Department of Chemistry, University at Buffalo, State University of New York, Buffalo, New York 14260, United States

Samantha N. MacMillan — Department of Chemistry and Chemical Biology, Cornell University, Ithaca, New York 14853, United States; orcid.org/0000-0001-6516-1823

Complete contact information is available at:

https://pubs.acs.org/10.1021/acs.organomet.1c00648

Author Contributions

§P.M.F. and V.V. contributed equally.

Notes

The authors declare no competing financial interest.

ACKNOWLEDGMENTS

Financial support was provided by the University at Buffalo (UB) and NSF CAREER award 1847933. This work utilized a Bruker SolariXR FT-ICRMS (purchased with NIH S10 RR029517) and a Thermo Scientific Q-Exactive GC-Orbitrap tandem MS (purchased with NSF CHE-1919594) at the UB Chemistry Instrument Center.

REFERENCES

- (1) Perutz, R. N.; Procacci, B. Photochemistry of transition metal hydrides. *Chem. Rev.* **2016**, *116*, 8506–8544.
- (2) Selected examples of M—H photolysis in catalysis: (a) Hoffman, N. W.; Brown, T. L. Thermal and photochemical substitution reactions of the tricarbonyl(cyclopentadienyl)hydrido compounds of tungsten and molybdenum. *Inorg. Chem.* 1978, 17, 613—617. (b) Yu, M. M.; Jing, H. Z.; Liu, X.; Fu, X. F. Visible-light-promoted generation of hydrogen from the hydrolysis of silanes catalyzed by rhodium(III) porphyrins. *Organometallics* 2015, 34, 5754—5758.
- (3) Example of light-induced M(H)₂ reductive elimination in catalysis: Schild, D. J.; Peters, J. C. Light enhanced Fe-mediated nitrogen fixation: mechanistic insights regarding H₂ elimination, HER, and NH₃ generation. ACS Catal. 2019, 9, 4286–4295.
- (4) Examples of photoinduced H₂ release from MH and acid: (a) Heyduk, A. F.; Nocera, D. G. Hydrogen produced from hydrohalic acid solutions by a two-electron mixed-valence photocatalyst. *Science* **2001**, 293, 1639–1641. (b) Pitman, C. L.; Miller, A. J. M. Molecular photoelectrocatalysts for visible light-driven hydrogen evolution from neutral water. *ACS Catal.* **2014**, *4*, 2727–2733.
- (5) Fast, C. D.; Schley, N. D. Light-promoted transfer of an iridium hydride in alkyl ether cleavage. *Organometallics* **2021**, *40*, 3291–3297.
- (6) Freixa, Z. Photoswitchable catalysis using organometallic complexes. Catal. Sci. Technol. 2020, 10, 3122-3139.
- (7) Fanara, P. M.; MacMillan, S. N.; Lacy, D. C. Planar-locked Ru-PNN catalysts in 1-phenylethanol dehydrogenation. *Organometallics* **2020**, 39, 3628–3644.
- (8) Gusev, D. Revised mechanisms of the catalytic alcohol dehydrogenation and ester reduction with the Milstein PNN complex of ruthenium. *Organometallics* **2020**, *39*, 258–270.
- (9) He, T.; Buttner, J. C.; Reynolds, E. F.; Pham, J.; Malek, J. C.; Keith, J. M.; Chianese, A. R. Dehydroalkylative activation of CNN- and PNN-pincer ruthenium catalysts for ester hydrogenation. *J. Am. Chem. Soc.* **2019**, *141*, 17404–17413.
- (10) Dawe, L. N.; Karimzadeh-Younjali, M.; Dai, Z.; Khaskin, E.; Gusev, D. G. The Milstein bipyridyl PNN pincer complex of ruthenium becomes a Noyori-type catalyst under reducing conditions. *J. Am. Chem. Soc.* **2020**, *142*, 19510–19522.
- (11) Sordakis, K.; Tang, C.; Vogt, L. K.; Junge, H.; Dyson, P. J.; Beller, M.; Laurenczy, G. Homogeneous catalysis for sustainable hydrogen storage in formic acid and alcohols. *Chem. Rev.* **2018**, *118*, 372–433.
- (12) Gunanathan, C.; Milstein, D. Metal-ligand cooperation by aromatization-dearomatization: a new paradigm in bond activation and "green" catalysis. *Acc. Chem. Res.* **2011**, *44*, 588–602.
- (13) Crabtree, R. H. Homogeneous transition metal catalysis of acceptorless dehydrogenative alcohol oxidation: applications in hydrogen storage and to heterocycle synthesis. *Chem. Rev.* **2017**, *117*, 9228–9246.
- (14) (a) Trincado, M.; Banerjee, D.; Grützmacher, H. Molecular catalysts for hydrogen production from alcohols. *Energy Environ. Sci.* **2014**, *7*, 2464–2503. (b) Trincado, M.; Bösken, J.; Grützmacher, H.

Homogeneously catalyzed acceptorless dehydrogenation of alcohols: a progress report. *Coord. Chem. Rev.* **2021**, *443*, 213967.

- (15) Zhang, J.; Leitus, G.; Ben-David, Y.; Milstein, D. Facile conversion of alcohols into esters and dihydrogen catalyzed by new ruthenium complexes. *J. Am. Chem. Soc.* **2005**, *127*, 10840–10841.
- (16) Buhaibeh, R.; Filippov, O. A.; Bruneau-Voisine, A.; Willot, J.; Duhayon, C.; Valyaev, D. A.; Lugan, N.; Canac, Y.; Sortais, J.-B. Phosphine-NHC manganese hydrogenation catalyst exhibiting a non-classical metal-ligand cooperative H₂ activation mode. *Angew. Chem., Int. Ed.* **2019**, *58*, *6727*–*6731*.
- (17) Chakraborty, S.; Gellrich, R.; Diskin-Posner, Y.; Leitus, G.; Avram, L.; Milstein, D. Manganese-catalyzed N-formylation of amines by methanol liberating H₂: a catalytic and mechanistic study. *Angew. Chem., Int. Ed.* **2017**, *56*, 4229–4233.
- (18) Devillard, M.; Ehlers, A.; Siegler, M. A.; van der Vlugt, J. I. Selective carbanion—pyridine coordination of a reactive P,N ligand to Rh^I. Chem. Eur. J. 2019, 25, 3875—3883.
- (19) Werner, H.; Werner, R. J. Basic metals. *J. Organomet. Chem.* **1981**, 209, C60–C64.
- (20) At 110 $^{\circ}$ C in toluene with static vacuum, the free ligand, (CO) $\{PPh_3\}_3Ru^{II}(H)_2$, and 3 were observed in a nearly 1:1:1 ratio.
- (21) Ben-Ari, E.; Leitus, G.; Shimon, L. J. W.; Milstein, D. Metalligand cooperation in C–H and H_2 activation by an electron-rich PNP Ir(I) system: facile ligand dearomatization—aromatization as key steps. *J. Am. Chem. Soc.* **2006**, *128*, 15390–15391.
- (22) Procacci, B.; Duckett, S. B.; George, M. W.; Hanson-Heine, M. W. D.; Horvath, R.; Perutz, R. N.; Sun, X. Z.; Vuong, K. Q.; Welch, J. A. Competing pathways in the photochemistry of Ru(H)₂(CO)(PPh₃)₃. *Organometallics* **2018**, *37*, 855–868.
- (23) Geoffroy, G. L.; Denton, D. A.; Keeney, M. E.; Bucks, R. R. Photoinduced Oxidation of Coordinated Ligands in Trans-[RhCl-(CO)(PPh₃)₂]. Generation of a Decarbonylation Agent. *Inorg. Chem.* **1976**, *15*, 2382–2385.
- (24) Durham, B.; Wilson, S. R.; Hodgson, D. J.; Meyer, T. J. Cis-trans photoisomerization in Ru(bpy)₂(OH₂)²⁺. Crystal structure of *trans*-[Ru(bpy)₂(OH₂)(OH)](ClO₄)₂. *J. Am. Chem. Soc.* **1980**, 102, 600–607.
- (25) Meakin, P.; Muetterties, E. L.; Tebbe, F. N.; Jesson, J. P. Stereochemically nonrigid six-coordinate molecules. I. A detailed mechanistic analysis for the molecule $FeH_2[P(OC_2H_5)_3]_4$. *J. Am. Chem. Soc.* **1971**, 93, 4701–4709.
- (26) (a) Gusev, D. G.; Vymentis, A. B.; Bakhmutov, V. I. Is $RuH_4(PPh_3)_3$ in solution indeed a non-classical hydride? *Inorg. Chim. Acta* **1991**, *179*, 195–201. (b) Khalsa, G. R. K.; Kubas, G. J.; Unkefer, C. J.; van Der Sluys, L. S.; Kubat-Martin, K. A. Molecular hydrogen complexes of the transition metals. 7. Kinetics and thermodynamics of the interconversion between dihydride and dihydrogen forms of $W(CO)_3(PR_3)_2H_2$ where R = isopropyl and cyclopentyl. *J. Am. Chem. Soc.* **1990**, *112*, 3855–3860.
- (27) (a) See Table 2 in: Esswein, A. J.; Nocera, D. G. Hydrogen production by molecular photocatalysis. *Chem. Rev.* **2007**, *107*, 4022–4047. (b) Morton, D.; Cole-Hamilton, D. J.; Utuk, I. D.; Paneque-Sosa, M.; Lopez-Poveda, M. Hydrogen production from ethanol catalyzed by group 8 metal complexes. *J. Chem. Soc., Dalton Trans.* **1989**, 489.
- (28) (a) Lorusso, P.; Ahmad, S.; Brill, K.; Cole-Hamilton, D. J.; Sieffert, N.; Bühl, M. On the catalytic activity of [RuH₂(PPh₃)₃(CO)] (PPh₃=triphenylphosphine) in ruthenium-catalysed generation of hydrogen from alcohols: a combined experimental and DFT study. *ChemCatChem.* **2020**, *12*, 2995–3009. (b) Pandey, A. M.; Digrawal, N. K.; Mohanta, N.; Jamdade, A. B.; Chaudhari, M. B.; Bisht, G. S.; Gnanaprakasam, B. Catalytic acceptorless dehydrogenation of amino alcohols and 2-hydroxybenzyl alcohols for annulation reaction under neutral conditions. *J. Org. Chem.* **2021**, *86*, 8805–8828.
- (29) Geoffroy, G. L.; Bradley, M. G. L. Photochemistry of transition metal hydride complexes. 2. Chlorohydro(carbonyl)tris-(triphenylphosphine)ruthenium, dihydro(carbonyl)tris-(triphenylphosphine)ruthenium, and chlorohydro(dicarbonyl)bis-(triphenylphosphine)ruthenium. *Inorg. Chem.* 1977, 16, 744–748.

- (30) See the Supporting Information for figures and methods detailing product identification and quantification.
- (31) Tseng, K.-N. T.; Kampf, J. W.; Szymczak, N. K. Mechanism of N,N,N-amide ruthenium(II) hydride mediated acceptorless alcohol dehydrogenation: inner-sphere β -H elimination versus outer-sphere bifunctional metal-ligand cooperativity. ACS Catal. 2015, 5, 5468– 5485
- (32) Fuse, H.; Mitsunuma, H.; Kanai, M. Catalytic acceptorless dehydrogenation of aliphatic alcohols. *J. Am. Chem. Soc.* **2020**, *142*, 4493–4499.
- (33) Zhong, J.-J.; To, W.-P.; Liu, Y.; Lu, W.; Che, C.-M. Efficient acceptorless photo-dehydrogenation of alcohols and *N*-heterocycles with binuclear platinum(II) diphosphite complexes. *Chem. Sci.* **2019**, 10, 4883–4889.
- (34) Brereton, K. R.; Bonn, A. G.; Miller, A. J. M. Molecular photoelectrocatalysts for light-driven hydrogen production. *ACS Energy Lett.* **2018**, *3*, 1128–1136.
- (35) Wang, W.; Rauchfuss, T. B.; Bertini, L.; Zampella, G. Unsensitized photochemical hydrogen production catalyzed by diiron hydrides. *J. Am. Chem. Soc.* **2012**, *134*, 4525–4528.
- (36) Whittemore, T. J.; Xue, C.; Huang, J.; Gallucci, J. C.; Turro, C. Single-chromophore single-molecule photocatalyst for the production of dihydrogen using low-energy light. *Nat. Chem.* **2020**, *12*, 180–185.
- (37) Huckaba, A. J.; Shirley, H.; Lamb, R. W.; Guertin, S.; Autry, S.; Cheema, H.; Talukdar, K.; Jones, T.; Jurss, J. W.; Dass, A.; Hammer, N. I.; Schmehl, R. H.; Webster, C. E.; Delcamp, J. H. A mononuclear tungsten photocatalyst for H₂ production. *ACS Catal.* **2018**, *8*, 4838–4847.
- (38) Nielsen, M.; Alberico, E.; Baumann, W.; Drexler, H.-J.; Junge, H.; Gladiali, S.; Beller, M. Low-temperature aqueous-phase methanol dehydrogenation to hydrogen and carbon dioxide. *Nature* **2013**, 495, 85–89.
- (39) (a) Oldenhuis, N. J.; Dong, V. M.; Guan, Z. Catalytic acceptorless dehydrogenations: Ru-MACHO catalyzed construction of amides and imines. *Tetrahedron* **2014**, *70*, 4213–4218. (b) Bertoli, M.; Choualeb, A.; Lough, A. J.; Moore, B.; Spasyuk, D.; Gusev, D. G. Osmium and ruthenium catalysts for dehydrogenation of alcohols. *Organometallics* **2011**, *30*, 3479–3482.
- (40) Fanara, P. M.A Study of Aromatization/Dearomatization Metal-Ligand Cooperativity with Ruthenium(II)-based PNN and PN Complexes, Chapter S. Ph.D. Dissertation, University at Buffalo, State University of New York, Buffalo, NY, 2021.